Journal of Power Sources 231 (2013) 301–306

Contents lists available at SciVerse ScienceDirect

Journal of Power Sources

journal homepage: www.elsevier.com/locate/jpowsour

Composite blend polymer membranes with increased proton selectivity and lifetime for vanadium redox flow batteries

Dongyang Chen [a], Soowhan Kim [b,**,1], Vincent Sprenkle [b], Michael A. Hickner [a,*]

[a] Department of Materials Science and Engineering, The Pennsylvania State University, University Park, PA 16802, USA
[b] Pacific Northwest National Laboratory, Richland, WA 99352, USA

HIGHLIGHTS

- ► Compatible blends of ionic polymer and reinforcing polymer are demonstrated.
- ► Proton selectivity and high conductivity improve cell efficiency.
- ► Composite VRFBs show longer-life device performance.
- ► Both chemical and mechanical degradation mitigated with new VRFB membrane design.

ARTICLE INFO

Article history:
Received 5 August 2012
Received in revised form
10 November 2012
Accepted 1 January 2013
Available online 9 January 2013

Keywords:
Vanadium redox flow battery
Proton exchange membrane
Blend
Composite
Selectivity

ABSTRACT

Composite membranes based on blends of sulfonated fluorinated poly(arylene ether) (SFPAE) and poly(vinylidene fluoride-co-hexafluoropropene) (P(VDF-co-HFP)) were prepared with varying P(VDF-co-HFP) content for vanadium redox flow battery (VRFB) applications. The properties of the SFPAE-P(VDF-co-HFP) blends were characterized by atomic force microscopy, differential scanning calorimetry, and Fourier transform infrared spectroscopy. The water uptake, mechanical properties, thermal properties, proton conductivity, VO^{2+} permeability and VRFB cell performance of the composite membranes were investigated in detail and compared to the pristine SFPAE membrane. It was found that SFPAE had good compatibility with P(VDF-co-HFP) and the incorporation of P(VDF-co-HFP) increased the mechanical properties, thermal properties, and proton selectivity of the materials effectively. An SFPAE composite membrane with 10 wt.% P(VDF-co-HFP) exhibited a 44% increase in VRFB cell lifetime as compared to a cell with a pure SFPAE membrane. Therefore, the P(VDF-co-HFP) blending approach is a facile method for producing low-cost, high-performance VRFB membranes.

1. Introduction

Vanadium redox flow battery (VRFB) technology has received significant interest recently as one of the most promising types of flow batteries for large-scale energy storage applications [1–3]. A VRFB device has a simple configuration consisting of porous or channeled carbon electrodes, an anolyte/catholyte separator, and externally supplied electrolytes that allow flexible, modular design for a wide range of power and energy storage requirements. Successes have been achieved for increasing the performance of flow batteries with highly active electrodes [4] and high stability electrolytes [5]; however, lack of cost-effective separators with both low resistance and low electrolyte permeation are limiting the commercialization of VRFB devices [6]. For the most studied type of VRFB separator, namely proton exchange membranes (PEM), the resistance parameter is expressed as proton conductivity (σ) while the electrolyte permeation parameter is expressed as VO^{2+} permeability (P). These two parameters are usually found to have a trade-off relationship, which must be taken into account in new materials design [7]. Therefore, the proton selectivity (defined as σ/P) becomes an important parameter for rational membrane design in these types of systems while keeping in mind that the conductivity must still remain high enough for effective device performance.

Nafion® is the benchmark PEM for many electrochemical applications because of its high proton conductivity under hydrated conditions and good oxidative stability during long-term operation, however; Nafion®'s proton selectivity is low when used in a VRFB

* Corresponding author. Tel.: +1 814 867 1847; fax: +1 814 865 2917.
** Corresponding author. Tel.: +1 509 371 6658; fax: +1 509 375 4448.
E-mail addresses: soowhankim@gmail.com (S. Kim), hickner@matse.psu.edu, mah49@psu.edu (M.A. Hickner).
[1] Current address: OCI Company Ltd. R&D Center 358-11, Sangdaewon1-dong, Jungwon-gu, Seongnam-si, Gyeonggi-do 462-807, Korea.

0378-7753/$ – see front matter © 2013 Elsevier B.V. All rights reserved.
http://dx.doi.org/10.1016/j.jpowsour.2013.01.007

due to its high vanadium ion permeability, leading to low coulombic efficiency of the cell and rapid capacity fade with cycling [8,9]. Various Nafion®-based composite membranes have been prepared with an aim to increase the proton selectivity by decreasing the VO^{2+} permeability significantly while maintaining the proton conductivity at a relatively high level. Successful examples include organic–inorganic hybrid membranes of Nafion® and SiO_2 [10–12] or TiO_2 [13,14], organic–organic blend membranes of Nafion® and poly(vinylidene fluoride) [15] or sulfonated poly(arylene ether)s [16,17]. While these composite membranes can show improved cell performance in VRFB cells, Nafion® is currently too expensive for large-scale devices, so the modification of Nafion® do not address the root economic problems of the material.

As one of the most promising alternative PEMs to Nafion®, sulfonated poly(arylene ether)s (SPEs) were adopted to serve as low cost, high performance separators in VRFBs [18–21]. The proton conductivity of SPEs is difficult to increase to the same level as Nafion® unless much higher ion exchange capacity (IEC) is used. However, the VO^{2+} permeability is usually much lower than Nafion® for SPEs with moderate or low IECs, presumably because Nafion® has larger hydrophilic channels for the migration of VO^{2+} compared to smaller channels in SPEs [22]. Consequently, SPEs generally display higher proton selectivity than Nafion® in VRFB applications. It was found that careful modification of SPEs such as hybridizing with SiO_2 [23] or WO_3 [24] leads to even greater proton selectivity and cell performance, making SPEs one of the best choices for ion-conducting membranes as VRFB separators.

Our previous examination of sulfonated Radel® demonstrated that this aromatic ion-conducting polymer could not meet the long-term operation requirement of VRFBs due to degradation of the membrane upon cycling [25]. Fortunately, partially fluorinated aromatic proton exchange membranes were found to have much higher oxidative stability as evidenced by both *in situ* [7] and *ex situ* [26] measurements. Based on our previous IEC-optimized stable sulfonated fluorinated poly(arylene ether) (SFPAE) membrane (Scheme 1) [7], herein, we report our ongoing efforts to increase the proton selectivity and lifetime of the membrane by blending SFPAE with varying amounts of poly(vinylidene fluoride-co-hexafluoropropene) (P(VDF-co-HFP)).

2. Experimental

2.1. Materials

Sulfonated fluorinated poly(arylene ether) (SFPAE) with an ion exchange capacity (IEC) of 1.80 mequiv. g^{-1} was synthesized according to our previous report [7]. Nafion® NR212 was purchased from Ion Power Inc., USA. Poly(vinylidene fluoride-co-hexafluoropropene) (P(VDF-co-HFP), $M_w \sim 455$ kDa) was purchased from Sigma Aldrich Co., LLC. All the other reagents were purchased from common commercial suppliers and used without further purification.

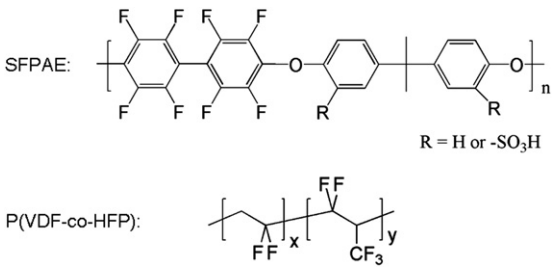

Scheme 1. Chemical structures of SFPAE and P(VDF-co-HFP).

2.2. Preparation of composite membranes

Composite membranes of SFPAE with 5 wt.%, 10 wt.%, 15 wt.%, 20 wt.% and 25 wt.% P(VDF-co-HFP) were prepared by solution casting. SFPAE and P(VDF-co-HFP) were mixed at the desired weight ratios and dissolved in N,N′-dimethylacetamide at approximately 8 wt./vol. %, followed by ultrasonic dispersion for 30 min. The polymer solutions were then cast onto glass plates, dried at 80 °C for 24 h, and then dried at 120 °C *in vacuo* for 24 h. The membranes were removed from the casting plate and immersed in a 1 M H_2SO_4 solution at 80 °C for 1 h. After acidification, the membranes were washed continuously with deionized water at 80 °C until the successive wash solutions were neutral (pH 7.0). The membranes were then stored in deionized water at room temperature for further characterization. The composite membranes were denoted as SFPAE-X, where X is the weight percent of P(VDF-co-HFP). For example, SFPAE-10% is a composite membrane of 90 wt.% SFPAE and 10 wt.% P(VDF-co-HFP).

2.3. Characterization

Fourier transform infrared spectroscopy (FTIR) spectra were recorded on a Bruker Vertex FTIR spectrometer with an MCT detector. Differential scanning calorimetry (DSC) was performed on a Q100 DSC (TA instruments Corp., USA) at a heating/cooling rate of 10 °C min^{-1} under N_2 atmosphere. Samples were first heated to 190 °C, cooled to 30 °C and then heated to 190 °C again. Data were collected from the second heating step. Thermal stability of the polymers was analyzed using a Q50 TGA (TA Instruments Corp., USA). The temperature was increased from room temperature to 120 °C and held for 30 min, and then increased to 800 °C at a heating rate of 10 °C min^{-1} under N_2 atmosphere. The mechanical properties were measured on an Instron 5866 Universal Testing Machine at room temperature. The microscopic morphology was examined by a Dimension FastScan® Atomic Force Microscope (Bruker AXS Inc., USA).

The ion exchange capacity (IEC) was measured by titration. Dried membrane was first weighed and immersed in a 1 M Na_2SO_4 solution for 24 h to deprotonate the sulfonic acid groups and form their corresponding sodium salt. The resulting solution was titrated with a KOH solution (0.1 M) using phenolphthalein pH indicator until the colorimetric endpoint. The IEC was calculated as the moles of exchangeable protons per gram of polymer membrane.

The water uptake of the membranes was defined as the weight ratio of the absorbed water to that of the dry membrane. The swelling ratio was described as the linear expansion ratio of wet membrane compared to its dry dimension. The proton conductivities of membranes were measured by two-probe electrochemical impedance spectroscopy (EIS) using a Solartron 1260A frequency response analyzer coupled to a Solartron 1287 potentiostat as previously reported [7]. The measurements were conducted while the cell was submerged in deionized water at room temperature (22 °C). The conductivity (σ) was calculated from the impedance plot according to the area available for membrane conducting (A) and the distance between the electrodes (d), $\sigma = d/RA$, where the resistance R was derived from the intercept of the high frequency complex impedance with the Re (Z') axis.

The VO^{2+} permeability measurement was conducted in a membrane-separated cell by filling 20 mL of 1.7 M $VOSO_4$ in 2.5 M H_2SO_4 solution into one reservoir and 20 mL of 1.7 M $MgSO_4$ in 2.5 M H_2SO_4 solution in the other reservoir. The two solutions were magnetically stirred at room temperature throughout the experiment. Samples of the $MgSO_4$ solution were taken at a regular time intervals and the concentration of VO^{2+} was measured with a VARIAN Cary 100 Scan UV–Visible spectrophotometer. The VO^{2+} permeability (P) was calculated from:

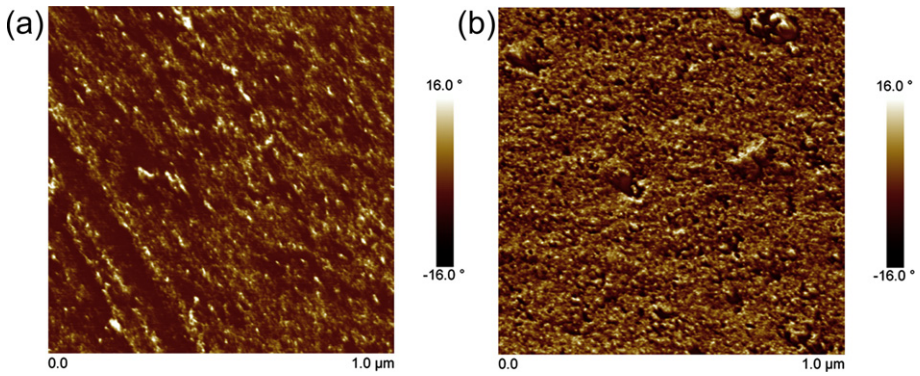

Fig. 1. AFM phase images of SFPAE (a) and representative composite membrane SFPAE-10% (b).

$$V_B \frac{dC_B(t)}{dt} = A\frac{P}{L}(C_A - C_B(t)) \quad (1)$$

where V_B is the volume of $MgSO_4$ solution, C_B is the concentration of permeated VO^{2+} ion in the $MgSO_4$ compartment, t is time, A is membrane area, L is membrane thickness, and C_A is the initial concentration of $VOSO_4$ compartment which is 1.7 M in this case.

VRFB cell performance measurements were conducted with 50 mL of 1.7 M VO^{2+} in 3.3 M H_2SO_4 solution as the anolyte and 50 mL of 1.7 M V^{3+} in 3.3 M H_2SO_4 solution as the catholyte. Membrane thickness for all tests was 55–64 μm. The cell configuration was the same as our previous report [19]. The cell was charged to 90% state-of-charge (SOC) and discharged to 10% SOC at the current density of 100 mA cm^{-2}. The coulombic efficiency (CE), voltage efficiency (VE) and energy efficiency (EE) were calculated by:

$$CE = \frac{\int I_d dt}{\int I_c dt} \times 100\% \quad (2)$$

$$EE = \frac{\int V_d I_d dt}{\int V_c I_c dt} \times 100\% \quad (3)$$

$$VE = \frac{EE}{CE} \times 100\% \quad (4)$$

where I_d is the discharging current, I_c is the charging current, V_d is the discharging voltage, V_c is the charging voltage.

3. Results and discussion

3.1. Blend compatibility

Transparent composite membranes were obtained for all P(VDF-co-HFP) contents from 0 to 25 wt.%. The microscopic morphology of the composite membranes was examined by tapping mode AFM and compared to that of the pristine SFPAE membrane. As shown in Fig. 1, SFPAE exhibited a distinct phase separated morphology as represented by dark and light areas, which correspond to hydrophilic and hydrophobic phases, respectively [27]. After the incorporation of P(VDF-co-HFP), a significant reduction was observed in the individual dark and light areas that indicated a more compact and less phase separated morphology of the composite samples. This data indicates that P(VDF-co-HFP) was well dispersed in the SFPAE matrix and the hydrophilic domain size of the composite membranes was reduced compared to the pure SFPAE membrane.

DSC was used to probe the crystallization characteristics of the P(VDF-co-HFP) in the SFPAE matrix. It can be seen in Fig. 2 that pure P(VDF-co-HFP) had a broad doublet melting peak at around 145–165 °C, while there was no melting peak for P(VDF-co-HFP) observed in the composite membranes. It was reported that P(VDF-co-HFP) displayed melting behavior in blends with other aromatic ionomers such as sulfonated poly(ether ether ketone)s [28] or sulfonated poly(phthalazinone ether sulfone ketone)s [29] due to the incompatibility between for P(VDF-co-HFP) and those non-fluorinated polymers. The lack of P(VDF-co-HFP) aggregation to form large enough crystallites to be observed by melting measurements in our system demonstrates good compatibility of P(VDF-co-HFP) and SFPAE.

The interaction of SFPAE and P(VDF-co-HFP) was investigated by FTIR, Fig. 3. The peak of the C–F stretching band for P(VDF-co-HFP) was found at 1182 cm^{-1} while the principle C–F stretch for SFPAE was found at 1175 cm^{-1}. Interestingly, the peaks of C–F stretching for the composite membranes were located between these two wavenumbers at 1178 cm^{-1} for SFPAE-25% and at 1188 cm^{-1} for SFPAE-10%. Furthermore, the C–F deformation peak appeared at 880 cm^{-1} for P(VDF-co-HFP) in the spectra of composite membranes, but was slightly shifted to 881 cm^{-1} for SFPAE-25% and 882 cm^{-1} for SFPAE-10%. These shifts in key FTIR bands clearly demonstrated that there were strong interactions between SFPAE and P(VDF-co-HFP), which promoted blending and good compatibility between these two polymers as evidenced by AFM and DSC measurements.

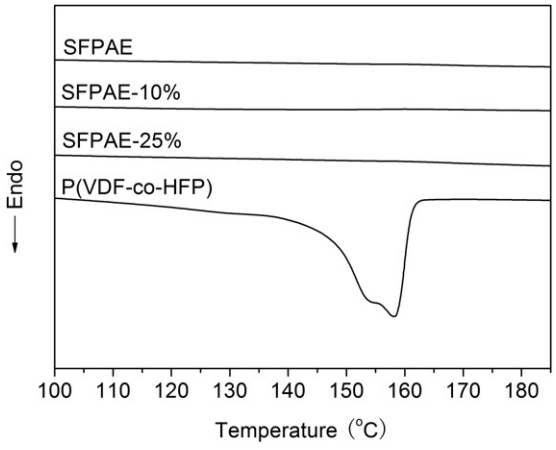

Fig. 2. DSC curves of P(VDF-co-HFP), SFPAE-25%, SFPAE-10% and SFPAE.

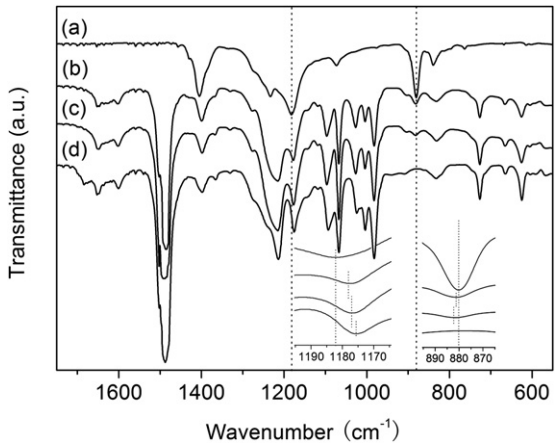

Fig. 3. FTIR spectra of (a) P(VDF-co-HFP); (b) SFPAE-25%; (c) SFPAE-10%; (d) SFPAE.

3.2. IEC, water uptake, and mechanical properties

From Table 1 the IEC of composite membranes decreased monotonically with increasing content of P(VDF-co-HFP). The ratio of the IEC of the composite membrane to the IEC of pristine SFPAE mirrored the weight content of SFPAE in the composite membrane. For example, the IEC of SFPAE-25% was 74% of the IEC of SFPAE, close to its SFPAE weight content of 75%. The water uptake and swelling ratio also decreased with an increased weight percent of P(VDF-co-HFP); however, these quantities decreased to a larger extent compared to what was anticipated from the SFPAE weight percent. For example, the water uptake of SFPAE-25% was only 57% of the water uptake of SFPAE while the sample had 75% SFPAE content. Thus, there is excess reinforcement of the composite membrane as promoted by the compatibility of the blend constituents.

Both the yield stress and yield strain increased with increasing weight percent of P(VDF-co-HFP), Fig. 4. The water uptake had an important effect on mechanical properties when the samples were fully hydrated [7]. Therefore, with increasing content of P(VDF-co-HFP), suppressed water uptake contributed to the increase in both yield stress and yield strain. However, the altered morphology and strong interaction between SFPAE and P(VDF-co-HFP) may also play a role in the increase in mechanical properties.

3.3. Thermal properties

The thermal stability of the composite membranes was investigated by thermogravimetric analysis (TGA) and compared to pristine SFPAE and P(VDF-co-HFP), Fig. 5. Pure SFPAE and the composite samples all showed a two-step decomposition profile typical of sulfonated ionomers [20], where the first step was the decomposition of sulfonic acid group and the second step was the decomposition of polymer backbone. Since the decompositions of SFPAE backbone and P(VDF-co-HFP) were in the same temperature range, they were overlapped for the composite membranes. It can be seen that the incorporation of P(VDF-co-HFP) slightly increased the temperature of the first decomposition step. All the samples were highly thermal stable for VRFB applications where the operation temperature is usually lower than 60 °C [18].

Table 1
Properties of SFPAE and composite membranes.

Sample	IEC (mequiv. g^{-1})	Water uptake (%)	Swelling ratio (%)	Proton conductivity (mS cm^{-1})
SFPAE	1.80	42	20	60
SFPAE-5%	1.73	39	19	59
SFPAE-10%	1.61	35	17	53
SFPAE-15%	1.55	32	14	49
SFPAE-20%	1.42	28	10	43
SFPAE-25%	1.34	24	8	34

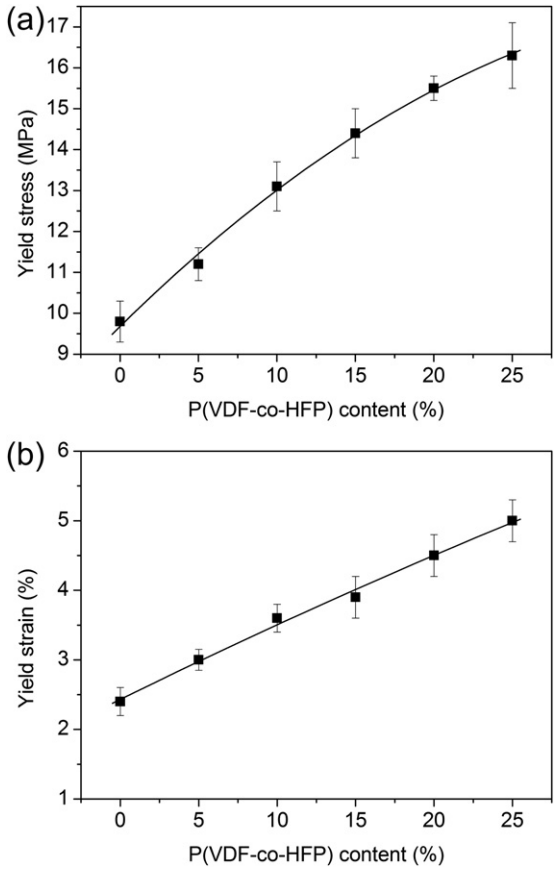

Fig. 4. (a) Yield stress and (b) yield strain of SFPAE and composite membranes.

3.4. Proton selectivity

The proton conductivity of the composite membranes decreased with the increasing content of P(VDF-co-HFP), Table 1. This trend was due to the correlation of both the IEC and water uptake with proton conductivity. As discussed above, the IEC and water uptake

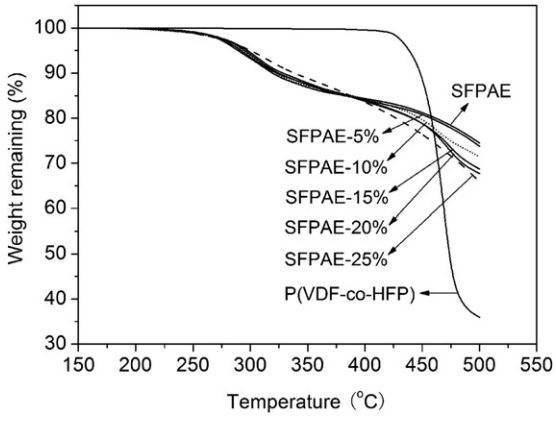

Fig. 5. TGA curves of SFPAE, P(VDF-co-HFP) and composite membranes.

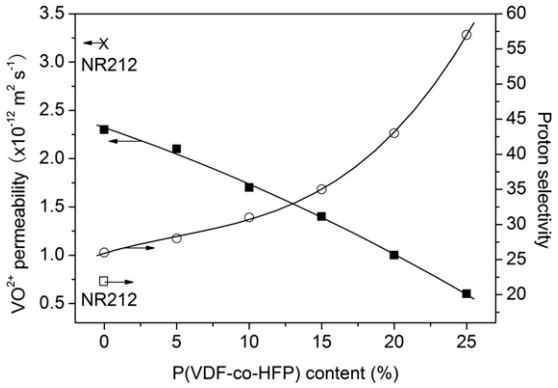

Fig. 6. VO^{2+} permeability and proton selectivity of SFPAE, NR212 and composite membranes.

decreased with the increasing content of P(VDF-co-HFP); therefore blending in inert polymer could be expected to result in decreased proton conductivity in the composite samples.

Blending of the SFPAE with P(VDF-co-HFP) decreased the VO^{2+} permeability of the membranes, Fig. 6. Because the VO^{2+} permeability decreased to a greater extent than the proton conductivity decreased with blending, Fig. 6 shows that the composite membranes had higher proton selectivity compared to the pure SFPAE sample. The increase in selectivity of aromatic proton exchange membranes relative to Nafion® has been observed in direct methanol fuel cell research [30,31]. Aromatic proton exchange membranes have small ionic domains which decreases the diffusion of water and small molecules without too large of a sacrifice in proton conductivity. Nafion®'s large ionic domains yield high conductivity, but also high water transport and small molecule diffusion [32].

3.5. Cell performance

High proton selectivity of the separator membrane is indispensable for high coulombic efficiency and long cycle life VRFB devices; however, low resistance (high proton conductivity in this case) of the membrane is also necessary for high power density output of the cell. To compromise between proton selectivity and conductivity, SFPAE-10% was selected for cell performance evaluations.

Previously, we evaluated the cell performance of IEC-optimized SFPAE membranes under different current densities and obtained higher CE, VE, and EE of the cell with the SFPAE membrane compared to a VRFB with a NR212 membrane [7]. While the *ex situ* vanadium soaking test demonstrated good stability of SFPAE membranes, long term cell cycling tests encountered membrane mechanical breakage, which became more severe under higher current densities. We believe degradation in aromatic proton exchange membranes in VRFBs is due to a small amount of chemical degradation of the polymer backbone [25]. This chemical degradation that was not obvious in the static soaking tests led to a significant decrease in mechanical strength of the membrane and a mechanically-based failure in post-test analyses. In order to evaluate the lifetime improvement of the composite membrane with better mechanical properties compared to the pristine SFPAE membrane, we evaluated the cycling performance of a cell under 100 mA cm^{-2} and the results are shown in Fig. 7 (single cycle charge–discharge curves), Table 2 (CE/VE/EE from Fig. 7) and Fig. 8 (energy efficiency changes versus cycle number). It can be seen in Fig. 7 that the charge–discharge behaviors of VRFBs assembled with SFPAE and SFPAE-10% were similar. The high frequency resistance (HFR) of the VRFB assembled with SFPAE was 0.35 Ω cm^{-2} while that of VRFB assembled with SFPAE-10% was 0.44 Ω cm^{-2}, slightly higher than the pure SFPAE membrane because of the slightly lower proton conductivity of SFPAE-10% compared to SFPAE. As a result, the VRFB assembled with SFPAE-10% exhibited slightly lower VE than the VRFB assembled with SFPAE, as shown in Table 2. Since SFPAE-10% had lower VO^{2+} permeability and higher proton selectivity than SFPAE, the VRFB assembled with SFPAE-10% showed slightly higher CE than the VRFB assembled with SFPAE. While this single cycle cell performance of the VRFBs assembled with these two membranes was similar, the long term operation revealed a large difference in cycling lifetime as shown in Fig. 8. It can be seen that the SFPAE only survived for 52 cycles under this harsh condition while SFPAE-10% lasted for 75 cycles, a 44% improvement in lifetime due to reinforcement of the P(VDF-co-HFP) in the blend. This data indicates that mechanical reinforcement is an important strategy for improving the cycling lifetime of ion-containing polymers for VRFBs.

Table 2
CE, VE and EE of VRFBs assembled with SFPAE and SFPAE-10% membranes.

Sample	CE (%)	VE (%)	EE (%)
SFPAE	99.3	88.4	87.8
SFPAE-10%	99.4	88.2	87.7

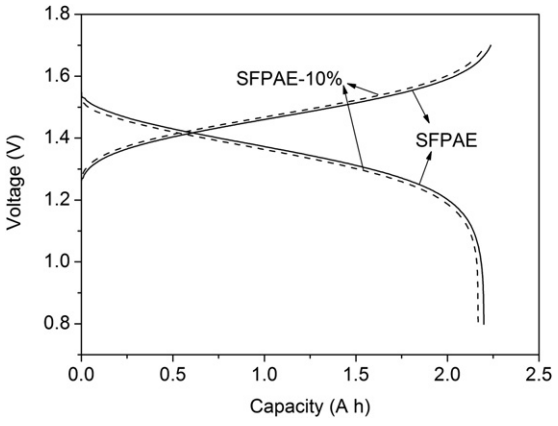

Fig. 7. Charge–discharge curves of VRFBs assembled with SFPAE and SFPAE-10% at 100 mA cm^{-2}.

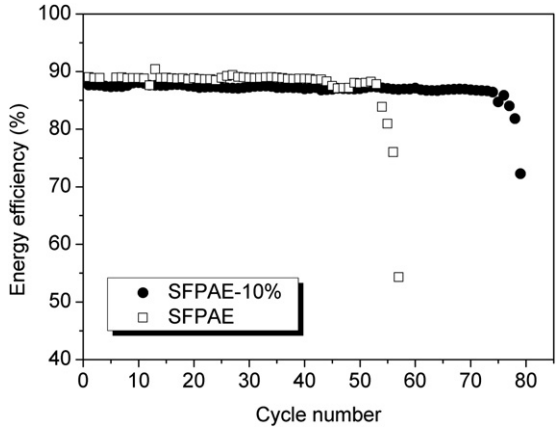

Fig. 8. Cycling performance of VRFBs assembled with SFPAE and SFPAE-10% at 100 mA cm^{-2}.

4. Conclusions

Composite blend proton exchange membranes of sulfonated fluorinated poly(arylene ether) (SFPAE) and poly(vinylidene fluoride-co-hexafluoropropene) (P(VDF-co-HFP)) were successfully prepared by solution casting with various contents of P(VDF-co-HFP). Strong intermolecular interactions between SFPAE and P(VDF-co-HFP) were evident from FTIR measurements. Good compatibility of these two polymers was found for all P(VDF-co-HFP) contents studied (5–25 wt.%) as indicated by the homogeneous atomic force micrographs and no P(VDF-co-HFP) crystallinity in DSC measurements. The incorporation of P(VDF-co-HFP) in a SFPAE membrane increased the mechanical properties, thermal stability, and proton selectivity effectively. A SFPAE membrane with 10 wt % P(VDF-co-HFP) had a good balance of proton conductivity and proton selectivity and was chosen for VRFB testing. Longer lifetime and slightly higher CE was achieved for the VRFB with a blend membrane as compared to the VRFB with a pristine SFPAE membrane. Through this work, blending an ionic polymer with a reinforcing polymer is a facile method for producing high performance, low cost VRFB membranes.

Acknowledgments

The work was supported by the Office of Electricity (OE Delivery & Energy Reliability (OE)), U.S. Department of Energy (DOE) under contract DE-AC05-76RL01830.

References

[1] M. Skyllas-Kazacos, G. Kazacos, G. Poon, G. Verseema, Int. J. Energy Res. 34 (2010) 182–189.
[2] Z. Weber, M.M. Mench, J.P. Meyers, P.N. Ross, J.T. Gostick, Q.H. Liu, J. Appl. Electrochem. 41 (2011) 1137–1164.
[3] B. Schwenzer, J.L. Zhang, S.W. Kim, L.Y. Li, J. Liu, Z.G. Yang, ChemSusChem 4 (2011) 1388–1406.
[4] K.J. Kim, M.S. Park, J.H. Kim, U. Hwang, N.J. Lee, G. Jeong, Y.J. Kim, Chem. Commun. 48 (2012) 5455–5457.
[5] D. Zhang, Q. Liu, X. Shi, Y. Li, J. Power Sources 203 (2012) 201–205.
[6] X. Li, H. Zhang, Z. Mai, H. Zhang, I. Vankelecom, Energy Environ. Sci. 4 (2011) 1147–1160.
[7] D. Chen, S. Kim, L. Li, G. Yang, M.A. Hickner, RSC Adv. (2012). http://dx.doi.org/10.1039/c2ra20834b.
[8] B. Tian, C.W. Yan, F.H. Wang, J. Membr. Sci. 234 (2004) 51–54.
[9] J. Xi, Z. Wu, X. Teng, Y. Zhao, L. Chen, X. Qiu, J. Mater. Chem. 18 (2008) 1232–1238.
[10] P. Trogadas, E. Pinot, T.F. Fuller, Electrochem. Solid State Lett. 15 (2012) A5–A8.
[11] X. Teng, Y. Zhao, J. Xi, Z. Wu, X. Qiu, L. Chen, J. Power Sources 189 (2009) 1240–1246.
[12] X. Teng, J. Lei, X. Gu, J. Dai, Y. Zhu, F. Li, Ionics 18 (2012) 513–521.
[13] X. Teng, Y. Zhao, J. Xi, Z. Wu, X. Qiu, L. Chen, J. Membr. Sci. 341 (2009) 149–154.
[14] N. Wang, S. Peng, D. Lu, S. Liu, Y. Liu, K. Huang, J. Solid State Electrochem. 16 (2012) 1577–1584.
[15] Z. Mai, H. Zhang, X. Li, S. Xiao, H. Zhang, J. Power Sources 196 (2011) 5737–5741.
[16] Q. Luo, H. Zhang, J. Chen, D. You, C. Sun, Y. Zhang, J. Membr. Sci. 325 (2008) 553–558.
[17] C. Jia, J. Liu, C. Yan, J. Power Sources 203 (2012) 190–194.
[18] D. Chen, S. Wang, M. Xiao, Y. Meng, J. Power Sources 195 (2010) 2089–2095.
[19] S. Kim, J. Yan, B. Schwenzer, J. Zhang, L. Li, J. Liu, Z. Yang, M.A. Hickner, Electrochem. Commun. 12 (2010) 1650–1653.
[20] D. Chen, S. Wang, M. Xiao, Y. Meng, Energy Environ. Sci. 3 (2010) 622–628.
[21] Z. Mai, H. Zhang, X. Li, C. Bi, H. Dai, J. Power Sources 196 (2011) 482–487.
[22] W. Wei, H. Zhang, X. Li, Z. Mai, H. Zhang, J. Power Sources 208 (2012) 421–425.
[23] D. Chen, S. Wang, M. Xiao, D. Han, Y. Meng, J. Power Sources 195 (2010) 7701–7708.
[24] N. Wang, S. Peng, H. Wang, Y. Li, S. Liu, Y. Liu, Electrochem. Commun. 17 (2012) 30–33.
[25] S. Kim, T.B. Tighe, B. Schwenzer, J. Yan, J. Zhang, J. Liu, Z. Yang, M.A. Hickner, J. Appl. Electrochem. 41 (2011) 1201–1213.
[26] D. Chen, M.A. Hickner, S. Wang, J. Pan, M. Xiao, Y. Meng, J. Membr. Sci. 415–416 (2012) 139–144.
[27] N. Li, S.Y. Lee, Y.L. Liu, Y.M. Lee, M.D. Guiver, Energy Environ. Sci. 5 (2012) 5346–5355.
[28] T.Y. Inan, H. Dogan, E.E. Unveren, E. Eker, Int. J. Hydrogen Energy 35 (2010) 12038–12053.
[29] S. Gu, G. He, X. Wu, Z. Hu, L. Wang, G. Xiao, L. Peng, J. Appl. Polym. Sci. 116 (2010) 852–860.
[30] M.A. Hickner, B.S. Pivovar, Fuel Cells 5 (2005) 213–229.
[31] J. Yan, X. Huang, H.D. Moore, C.-Y. Wang, M.A. Hickner, Int. J. Hydrogen Energy 37 (2012) 6153–6160.
[32] K.D. Kreuer, J. Membr. Sci. 185 (2001) 29–39.